Open
LETTER TO THE EDITOR

Cell Research (2017) 27:713-716.
www.nature.com/cr

Live cell single molecule-guided Bayesian localization super resolution microscopy

Cell Research (2017) **27**:713-716. doi:10.1038/cr.2016.160; published online 30 December 2016

Dear Editor,

Many current super resolution (SR) microscopic techniques [1-6] have been successfully applied to image cellular dynamics in living cells, but their applications have remained technically challenging. Live cell stimulated emission depletion (STED)/reversible saturable optical linear fluorescence transitions (RESOLFT) microscopy and structured illumination microscopy (SIM)/nonlinear SIM require sophisticated expensive optical setups and specialized expertise for accurate optical alignment. Live cell photo-activated localization microscopy (PALM)/stochastic optical reconstruction microscopy (STORM) use less complicated setup; however, a scientific complementary metal-oxide-semiconductor (sCMOS) camera, whose pixel-dependent noise must be characterized and calibrated before use [7], is required for extremely high acquisition speed over tens of thousands of frames. Recently, wide field-based SR microscopies have been developed to improve temporal resolution using much fewer time-lapse images (hundreds to thousands) than PALM/STORM [8, 9]. One of them, Bayesian analysis of the blinking and bleaching (3B) [8], offers enormous potential to resolve ultrastructure and fast cellular dynamics in living cells beyond the diffraction limit. Despite its potential, 3B analysis is impractical when imaging the nanoscale dynamics in large fields of view over long time periods, as the calculation is extremely time-consuming [8] and/or the analysis consumes large amounts of web resources [10]. Another major problem of 3B imaging is the artificial thinning and thickening of structures both in simulated image data and in experimental data [8, 10].

In the present study we first developed a Quick-3B algorithm, which can calculate 17-fold faster than 3B; however, it still artificially produces discontinuous dot-shaped structures (Supplementary information, Figure S1A). We therefore developed SIMBA (single molecule-guided Bayesian localization microscopy) to further improve the fidelity of the method, as well as the computation speed and temporal resolution by combining single molecule localization and other algorithms (Supplementary information, Data S1 and Figure S2). SIMBA can produce an appropriate 50 nm SR image of actin in fixed cells, and calculate a series of whole cell live structures with a 0.5-2 s temporal resolution for 50 time points on a desktop computer.

To validate that SIMBA can reconstruct an underlying SR structures, we labeled actin with lifeact-mEos3.2 in U2OS cells and performed correlative experiments. The actin network is highly dynamic and exhibits different subtype structures criss-crossing at various distances and angles, including stress fibers and bundles with different sizes and diameters [6]. To determine whether SIMBA can discriminate between these different structures, we compared the result of SIMBA analysis with that of 3B analysis and PALM imaging (Figure 1A-1C). A small area (15 × 30 pixels, 1 pixel = 160 nm) of actin ruffles (Figure 1A) was chosen for comparison because 3B analysis is impractical for calculating the entire field of view (Figure 1B1-6). Compared with 3B analysis, the actin ruffles produced by SIMBA analysis from 200 frames resembled more closely to the PALM data from 20 000 frames (Figure 1B4-6). Notably, the thin and discontinuous structures, artifacts seen in 3B analysis (Figure 1B2), were similar to what were previously reported [8]. These artifacts were absent in the images produced by SIMBA (Figure 1B3), Furthermore, unlike in 3B analysis, where the running time increases exponentially as the field of view (FOV) enlarges, the running time for different FOVs is nearly constant in SIMBA (Figure 1C1). Most strikingly, the larger the image areas are, the more advantage SIMBA has over the 3B analysis. For an area of 50 × 50 pixels, SIMBA's computing time was approximately 100 times shorter than that of the 3B analysis (Figure 1C2).

Encouraged by the superior computing speed and localization accuracy within small areas, we reconstructed a whole cell SR image of actin structures by SIMBA analysis using only 200 raw frames and compared the result with that made by PALM using 20,000 frames. The whole cell SIMBA image shows various distinct actin structures, such as actin filaments, actin bundles, and

ruffles, which are confirmed by PALM (Supplementary information, Figure S1B). An example is the ruffle structure resolved by the SIMBA analysis (Supplementary information, Figure S1B), which has very similar details as that resolved by PALM (Supplementary information, Figure S1B), with features separated by the same distances in both data sets (Supplementary information, Figure S1B). We determined the spatial resolution by measuring the distance at which two actin strands could be visually separated (Supplementary information, Figure S1B) and found that the SIMBA method achieved 49-nm resolution at an intersection of two strands (Supplemen-

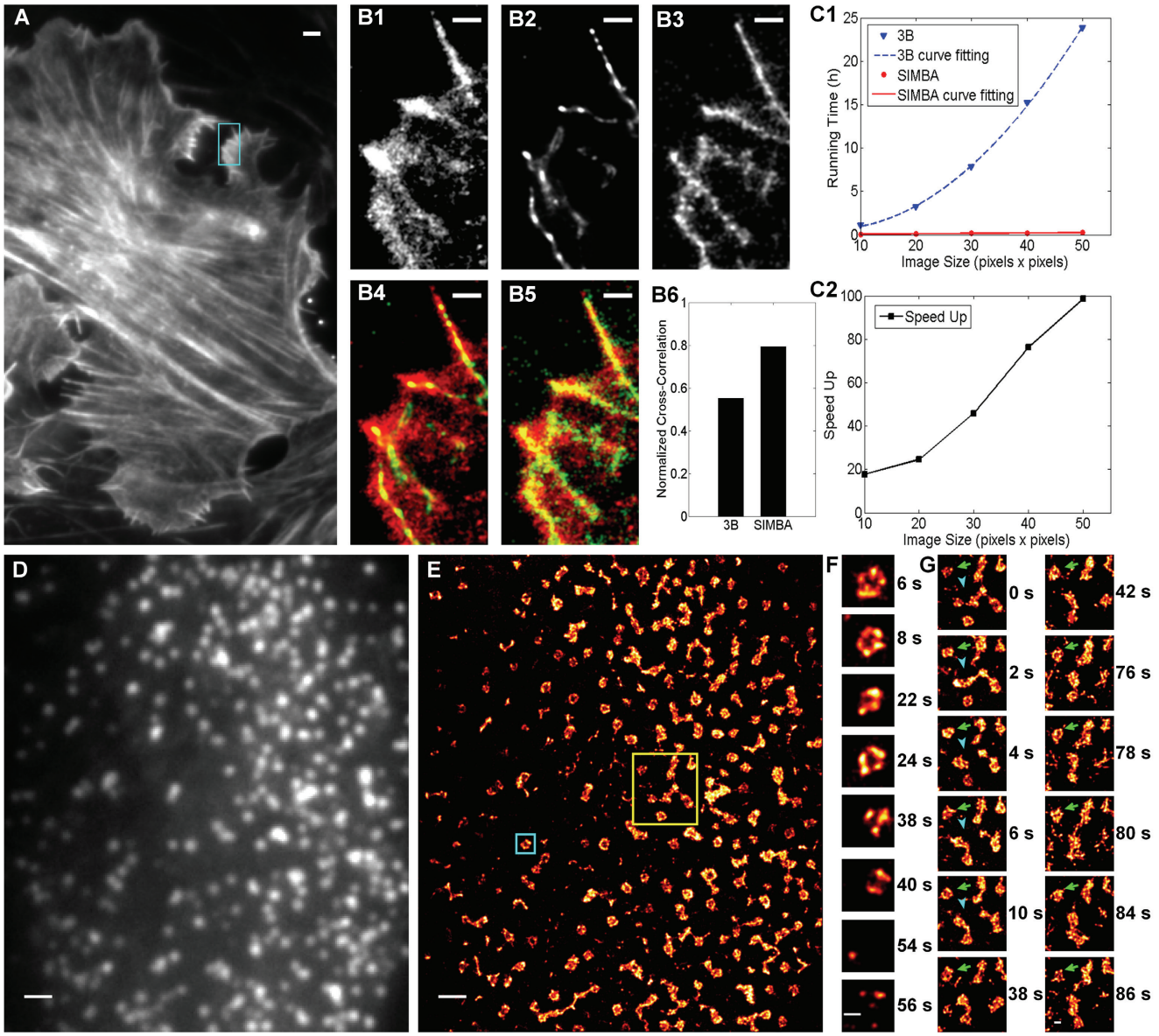

Figure 1 SIMBA imaging of actin network in a fixed U2OS cell and CCPs in a living HeLa cell. **(A)** Superimposed fluorescence data from the 200 TIRF frames in the SIMBA data set showing the diffraction limit resolution. **(B1-3)** Reconstruction of the actin ruffles indicated in the cyan box in **A** using PALM **(B1)**, 3B **(B2)** and SIMBA **(B3)**. **(B4)** Overlay of **B1** and **B2**. **(B5)** Overlay of **B1** and **B3**. **(B6)** Normalized cross correlation between 3B and PALM is 0.55, between SIMBA and PALM is 0.79. **(C1)** Computation time for 3B and SIMBA analysis of different image areas (10 × 10 pixels to 50 × 50 pixels). Blue dotted line: 3B; red solid line: SIMBA. **(C2)** Comparison of the speed of SIMBA and the speed of 3B for different imaging areas. **(D)** Diffraction limit image of mEos3.2-CLC (clathrin light chain) created by summing the first 100 TIRF frames. **(E)** The reconstructed SIMBA image of mEos3.2-CLC. **(F)** Time-lapse images at selective time points of region outlined by the cyan box in **E**. **(G)** Time-lapse images at selective time points of region outlined by the yellow box in **E**. Scale bars are 2 μm **(A)**, 1 μm **(D**, **E)**, 500 nm **(B1-5)** and 200 nm **(F**, **G)**.

tary information, Figure S1B). Also, by calculating the averaged half width at half maximum (FWHM) from a few thinnest filaments, we found the mean localization precision of SIMBA is 44 ± 5.6 nm (data not shown).

We next performed SR imaging of actin-based structures and clathrin-coated pits (CCPs) over large FOV in live cells by the SIMBA analysis. Lifeact-mEos3.2 was used to label the actin network in U2OS cells. A series of time-lapse images with an 18-ms exposure and a 20-s interval were acquired and each 100 frames were used to reconstruct one SR image by the SIMBA analysis. An example of the reconstructed results from the experiment is shown in the Supplementary information, Movie S1. Compared with the whole cell wide field image (Supplementary information, Figure S1C), the reconstructed SIMBA SR image showed much higher resolution and contained many more details (Supplementary information, Figure S1C). Highly dynamic movements of the actin network and the formation of actin ring structures were observed (Supplementary information, Figure S1C). To further increase the temporary resolution of the SIMBA method, we increased the acquisition speed and found that actin structures could still be well resolved at a 5-ms exposure time (Supplementary information, Movie S2), thus achieving a minimum acquisition time of 0.5 s.

Next we examined CCP formation in live Hela cells. As a control, the PALM images from 100 frames could not resolve the ring structures characteristic of CCPs due to low molecular density, neither could images from 5 000 frames that had much higher molecular density but reduced temporal resolution (Supplementary information, Figure S1D). On contrast, mature CCPs imaged at 37 °C can be successfully resolved as rings at one or more time points by the SIMBA method using the same 100 frames (Figure 1D-1G and Supplementary information, Movie S3). Both isolated rings and larger aggregates were observed, similar to the structures reported in COS-7 cells [6]. Most strikingly, CCPs resolved by SIMBA showed more complete and continuous structure than the previous live cell PALM result using high acquisition speed achieved by sCMOS [7]. Our time-lapse imaging showed that some mEos3.2-CCPs were dynamic, appearing and disappearing during the experiment (Figure 1F). More interestingly, we observed that in almost the same area, one CCP remained stationary for a long time, while other CCPs underwent dynamical reorganization — segregating into isolated rings and then associating with each other again (Figure 1G). These results suggest that CCPs are highly dynamic structures, assembling, disassembling, and interacting with each other.

We next applied SIMBA to image structures inside the cells, the ER and mitochondria, and found SIMBA could image intracellular structures with very high spatial resolution (Supplementary information, Figure S1E).

In summary, our study finds that Quick-3B analysis can greatly accelerate the computation speed of 3B. We next present a powerful live cell SR method, SIMBA, with several remarkable advantages. First, SIMBA is easy to use and is easy to combine with total internal reflection fluorescence microscope (TIRFM), PALM, STORM and light-sheet microscopy without any additional hardware and expertise. Second, it can achieve a 50 nm spatial resolution as judged by the measurement of actin structures in the fixed cells. Third, it requires much less computational resource compared with 3B and can be done on a desktop computer. Fourth, it extends the 3B technology to SR imaging of whole cells with a 0.5-2 s temporal resolution over a long observation period with significantly fewer image artifacts.

Acknowledgments

This project was supported by the National Basic Research Program (2013CB910103), the National Key Research and Development Projects (2016YFA0501500), the National Natural Science Foundation of China (31421002, 31370851, 31170818, 31300612, 61232001, 61472397, 61672493 and 61502455), Project of the Chinese Academy of Sciences (XDB08030202), Beijing Natural Science Foundation (7131011), Youth Innovation Promotion Association CAS (2012080 and 2013067) and Young Elite Scientist Sponsorship Program by CAST.

Competing Financial Interests

The SIMBA and the Quick-3B analysis algorithms as described here are covered within China provisional patent application 201610282305.5 filed by PX, FZ, FX and MZ and assigned to IBP.

Fan Xu[1, 2, 4, *], Mingshu Zhang[2, 3, *], Wenting He[2, 3], Renmin Han[1, 4, 5], Fudong Xue[2, 3, 4], Zhiyong Liu[1], Fa Zhang[1], Jennifer Lippincott-Schwartz[6], Pingyong Xu[2, 3, 7]

[1]Key Lab of Intelligent Information Processing, Institute of Computing Technology, Chinese Academy of Sciences, Beijing 100190, China; [2]Key Laboratory of RNA Biology, Institute of Biophysics, Chinese Academy of Sciences, Beijing 100101, China; [3]Beijing Key Laboratory of Noncoding RNA, Institute of Biophysics, Chinese Academy of Sciences, Beijing 100101, China; [4]Graduate School of the Chinese Academy of Sciences, University of Chinese Academy of Sciences, Beijing 100049, China; [5]Present address: Computational Bioscience Research Center, Computer, Electrical and Mathematical Sciences and Engineering Division, King Abdullah University of Science and Technology, Thuwal, 23955-6900, Kingdom of Saudi Arabia; [6]Janelia Research Campus, Howard Hughes Medical Institute, Ashburn, Virginia 20147, USA; [7]College of Life Sciences, University of Chinese Academy of Sciences, Beijing 100049, China

*These two authors contributed equally to this work.

Correspondence: Fa Zhang[a], Jennifer Lippincott-Schwartz[b], Pingyong Xu[c]

[a]E-mail: zhangfa@ict.ac.cn

[b]E-mail: lippincj@mail.nih.gov
[c]E-mail: pyxu@ibp.ac.cn

References

1 Kner P, Chhun BB, Griffis ER, *et al. Nat Methods* 2009; **6**:339-342.
2 Grotjohann T, Testa I, Reuss M, *et al. Elife* 2012; **1**:e00248.
3 Jones SA, Shim SH, He J, *et al*. *Nat Methods* 2011; **8**:499-508.
4 Westphal V, Rizzoli SO, Lauterbach MA, *et al*. *Science* 2008; **320**:246-249.
5 Shroff H, Galbraith CG, Galbraith JA, *et al*. *Nat Methods* 2008; **5**:417-423.
6 Li D, Shao L, Chen BC, *et al. Science* 2015; **349**:aab3500.
7 Huang F, Hartwich TMP, Rivera-Molina FE, *et al. Nat Methods* 2013; **10**:653-658.
8 Cox S, Rosten E, Monypenny J, *et al. Nat Methods* 2012; **9**:195-200.
9 Dertinger T, Colyer R, Iyer G, *et al*. *Proc Natl Acad Sci USA* 2009; **106**:22287-22292.
10 Hu YS, Nan X, Sengupta P, *et al*. *Nat Methods* 2013; **10**:96-97.

(**Supplementary information** is linked to the online version of the paper on the *Cell Research* website.)